Ideal superheating and supercooling limits in superconducting In and dilute *In*Bi alloys

Hugo Parr
Institute of Physics, University of Oslo, Blindern, Oslo 3, Norway
(Received 4 June 1976)

We have observed the ideal superheating and supercooling fields in 18-μm single spheres of In and *In*Bi (0.19, 0.395, and 0.60 at.%). Extrapolation of H_{sc}/H_c to $t = 1$ gives $\kappa(t = 1) = 0.061$, 0.155, 0.240, and 0.349, respectively, to an accuracy of 2%. The values of H_{sh}/H_c at $t = 1$ are 3.39, 2.44, 2.08, and 1.85, respectively, to 2% accuracy. These values are higher by 0%, 14%, 21%, and 30% than those given by the asymptotical expression $H_{sh} = H_c/(\kappa\sqrt{2})^{1/2}$, which is valid as $\kappa \to 0$. This is in fair agreement with one-dimensional Ginzburg-Landau theory for finite κ. Close to T_c, the hysteresis shrinks markedly as the tricritical point is approached. In the *In*Bi (0.60-at.%) sample, H_{sc} exceeded the demagnetizing field H_D, thus permitting observation of the intermediate state, the demagnetizing field H_D, and H_c. H_D shows a marked size effect, H_c almost none. In this sphere, the intermediate state can be made to superheat far beyond H_c. We interpret this as ideal superheating in the equatorial region, while a frozen-in normal domain is located along the polar axis.

I. INTRODUCTION

The superconductive superheating field in the Ginzburg-Landau (GL) approximation is given as[1,2]

$$H_{sh} = H_c/(\kappa\sqrt{2})^{1/2}, \tag{1}$$

which is valid asymptotically as $\kappa \to 0$. The very large superheating predicted by Eq. (1) was first seen in an In powder.[3] Later work on powders[4] and single spheres[5] have amply confirmed the GL prediction for low κ. For finite κ, numerical[1,6-8] and analytical[9] calculations have given a H_{sh} considerably larger than Eq. (1), but up till now this has not been tested experimentally with any precision, although some indications of an increase can be found in some of the earlier experiments.[10,11] The main purpose of this work is to establish H_{sh}/H_c for intermediate values of κ, and compare to the existing theory.

We chose the system of dilute *In*Bi alloys for a variety of reasons. These alloys are easy to make, and the low melting point of In makes it straightforward to produce flawless single spheres by sonoration. Ideal superheating and supercooling is easily obtained in In single spheres,[5] and was also seen in a preliminary investigation of *In*Bi powders.[12] T_c, H_0, and κ are all known to various degrees of accuracy as a function of composition.[12-14] We present separately (preceding paper[15]) the results of a simultaneous investigation of $\lambda(T, H)$ in the same alloys.

II. THEORY

A. Supercooling and superheating

Metastability of the normal phase in a decreasing field is limited in a perfect sample by homogeneous nucleation at the surface. This defines the supercooling field, which at T_c is given by[16]

$$H_{sc} = H_{c_3} = 1.695\sqrt{2}\,\kappa H_c. \tag{2}$$

This is valid for $\kappa < 0.409$. At lower temperatures, Eq. (2) is inverted to define the experimental parameter κ_{sc}:

$$\kappa_{sc}(t) = 0.4172\, H_{sc}/H_c. \tag{3}$$

At T_c, κ_{sc} equals the GL parameter κ, which is thus determined by extrapolation of the supercooling results to $t = 1$. This determines κ quite accurately, the limiting factor being the precision with which H_c is known. Ideal supercooling is readily obtained both in cylinders and spheres, and gives no problems of interpretation since there is no demagnetizing field.

Ideal superheating is much harder to produce. It has so far only been observed in spheres, either single[5,11] or in powders.[3,4,10,12] Large, but non-ideal, superheating has been seen in cylinders[17,18] and in an array of many thin-film squares.[19] For an infinite half-space in the GL approximation, we have recently extended Eq. (1) analytically to the next order in κ, obtaining[9]

$$H_{sh}/H_c = (1 + \tfrac{15}{32}\sqrt{2}\,\kappa)/(\kappa\sqrt{2})^{1/2} = (1 + 0.663\kappa)/(\kappa\sqrt{2})^{1/2}. \tag{4}$$

This agrees closely with numerical calculations[1,6-8] for $\kappa < 0.5$. At $\kappa = 1$, it gives a value of H_{sh} which is about 10% too high. The one-dimensional calculations of H_{sh} have been shown to be valid in three dimensions for $\kappa \leq 1.1$.[7] Equation (4) is therefore valid for all type-I materials close to T_c. Its validity, however, is limited by that of the GL theory itself to a temperature region $(1 - t) < \kappa^2$. For low-κ materials, this region is very small. At lower t, H_{sh} is given by the nonlocal expres-

sion[20]

$$H_{sh}/H_c = C(1-t)^{-1/12}\kappa^{-1/3}, \tag{5}$$

where $C \approx 0.8$–0.9 from experiments.[4] Note that substitution of $1-t=\kappa^2$ brings back Eq. (1) except for the numerical constant.

In the experimental determination of H_{sh}, the demagnetizing field of the sphere must be taken into account. The superheating transition will take place when the equatorial field H_{eq} reaches H_{sh}. For a sphere of finite penetration depth $\lambda(t) \cong \lambda_0 y$, $y=1/(1-t^4)^{1/2}$, the equatorial field is given by[21,22]

$$H_{eq} = H_{appl}k(T),$$
$$k(T) \cong \tfrac{3}{2}\,[1-\lambda_0 y/R + (\lambda_0 y/R)^2]. \tag{6}$$

For a precise determination of H_{sh}, it is important[11] to use the correct demagnetization coefficient $k(T)<\frac{3}{2}$. Otherwise, too high values of H_{sh} will result. For 18 μm spheres, the correction term in Eq. (16) is typically 0.97 at $t=0.99$ ($y\approx 5$), and 0.94 at $t=0.998$ ($y\approx 11$).

Close to T_c, when the coherence length $\xi(T)$ becomes of the order of R, a size effect sets in[1,5] which decreases the hysteresis. Thus, H_{sc} increases and H_{sh} decreases relative to the bulk values. Even closer to T_c, $\lambda(T)$ becomes of the order of R, and the transition changes from first to second order. In spheres, Ginzburg[1] found this changeover to take place when $R/\lambda(T)=\frac{1}{2}\sqrt{21}=2.29$. This may be called a tricritical point.[23] The dependence of H_{sc} and H_{sh} on R/λ has been computed numerically for films (Fig. 1 of Ref. 5) and cylinders.[24] For spheres, a good qualitative picture can be pieced together from the different limiting expressions of Ginzburg.[1] Experimentally, the shrinking and vanishing of the hysteresis as the tricritical point is approached, has been seen both in whiskers,[25] cylinders,[26] and films.[19] For 18 μm spheres, the size effect starts at $\Delta t \approx 1.5\times 10^{-2}$, and the tricritical point is at $\Delta t \approx 5\times 10^{-5}$, corresponding to a tricritical field of about 0.05 G. In our experiments, we reach $\Delta t \approx 2\times 10^{-4}$. Results are given in Sec. IV C.

B. Intermediate state in ellipsoids

To our knowledge, our measurements on the 17.8 μm *In*Bi (0.6-at.%) sphere (Sec. IV D) represent the first quantitative results on the intermediate state (IS) in small ellipsoids, as opposed to films and cylinders. Since Landau's pioneering work on the unbranched[27] and branched[28] models of the IS, subsequent theory and experiments have mostly dealt with the IS in films and plates. As a result, no "modern" thermodynamic treatment exists for the IS in ellipsoids.

In a large ellipsoid of demagnetizing factor n, the IS becomes thermodynamically favorable as the field reaches $H_D=(1-n)H_c^{bulk}$, and the normal state becomes favorable at H_c^{bulk}. In a small sample, the IS free energy increases because of the field distortion at the free surfaces. This leads to an increase in H_D and a decrease in H_c compared to the bulk values.[28,29] To get a feeling for the magnitude of these size effects, we have calculated from Landau's branched, laminar model[28] for an ellipsoid that:

$$\frac{H_D}{H_c} = (1-n) + \tfrac{5}{4}n\left(\frac{4}{\sqrt{2}-1}\,\frac{\Delta}{L}\right)^{0.4} - O((\Delta/L)^{0.8})\cdots . \tag{7}$$

For a sphere, $n=\frac{1}{3}$ and the characteristic length $L\approx R$. The surface-energy parameter $\Delta \approx 1.75\lambda(T)$ for $\kappa=0.35$.[30] Thus, Eq. (7) gives

$$H_D/H_c \approx \tfrac{2}{3} + 1.03[\lambda(T)/R]^{0.4}. \tag{8}$$

Andrew's branched thread model[29] gives a similar size effect in H_D, the exponent being 0.5 instead of 0.4. The size effect in H_c quite probably also gives a leading term in $(\lambda/R)^{1/2}$.[28,31] Since $(\lambda/R)^{1/2}\approx 0.18$ for 18 μm spheres at $t=0.99$, one would expect substantial size effects in both H_D and H_c. However, the above models are probably *not valid*. An improved theory might give an IS free energy with very different limiting properties close to H_c and H_D. Development of such a theory should probably start from the unbranched model, and use n, λ, and κ as parameters.

For interpretation of our data, we also need to know the characteristic size of an IS domain in a sphere. The domain periodicity is roughly given by a length[31]

$$D \approx [L\Delta/\phi(H)]^{1/2}. \tag{9}$$

Using $\phi_{max}\approx\frac{1}{4}$, $\Delta=1.75\lambda$, and $L\approx R$, we find for the *In*Bi (0.6-at.%) sphere that $D_{min}\approx 6$ μm at $t=0$, and ≈ 13 μm at $t=0.99$. Since the diameter is 17.8 μm, this means that very few domains will form, perhaps only one, probably along the polar axis.

III. EXPERIMENTAL

The *In* and[32] *In*Bi spheres were produced by ultrasonic dispersion of the molten metal in high-purity glycerol, to which was added 0.2% KOH by weight. The dispersion was quenched by pouring it into a mixture of equal proportions of glycerol and pure alcohol. The spheres were then repeatedly rinsed in alcohol. A drop containing many spheres was picked up with a soft brush and put on a microscope slide. After evaporation of the alco-

hol, spheres can be examined and handled under the microscope.[11] Spheres with flawless surfaces were picked, and their diameter determined to ± 0.5 μm.

The cryostat and detection system have been described before.[11,22] A germanium thermometer is used, calibrated to 5 mK accuracy against ^{4}He vapor pressure. Temperature can be stabilized to 0.1–0.2 mK and relative temperatures are known to this accuracy close to T_c, which is determined by a zero-field temperature sweep[33] to ± 0.2 mK. The correctness of this determination is independently verified by the measurements of the temperature dependence of the penetration depth. (Preceding paper,[15] Sec. IV A.) Our magnet is calibrated to 1% accuracy.

For most of the measurements, the 75-kHz tickling field was parallel to the static field, with a peak-to-peak amplitude of about 0.4–0.5 G. A small, transverse magnet was also available. Close to T_c, field sweeps were reversed so as to eliminate small axial remnant fields. The effect of a parallel tickling field is to linearly increase the measured H_{sc} and decrease H_{slr}; this was corrected for. In the size-effect region close to T_c, the tickling field was reduced by a factor of 5. Some experimental parameters are given in Table I.

IV. RESULTS AND DISCUSSION

A. T_c, $H_c(T)$, and resistance measurements

Relative values of T_c, given in Table I, are correct to ± 0.2 mK. They agree with previous measurements.[12] An initial decrease in T_c, due to smearing out of the anisotropy, is apparent. This effect probably peaks around 0.1-at.% Bi, and T_c is on its way up again at 0.19-at.% Bi, which is our first measuring point. In *In*Pb, the minimum in T_c occurs around a resistivity $\rho \approx 2\times 10^{-7}$ Ω cm.[34] Although we did not measure T_c for 0.1-at.% Bi, the resistance was measured, giving $\rho = 1.6\times 10^{-7}$ Ω cm, in excellent agreement with the *In*Pb results.

For interpretation of the superheating/supercooling results, an accurate knowledge of $H_c(T)$ is essential. For the three lower concentrations, the hysteresis was so large that the intermediate state, and thereby H_c, could not be observed. $H_c(T)$ was, however, measured for the *In*Bi 0.6-at.% sample (Sec. IV D). Experiments on *In*Pb dilute alloys[34] show that the difference in the deviation function $D(t^2)$ is negligible between these alloys and pure In. The only appreciable change occurs in H_0. Fitting our results using the deviation function of In:

$$D(t^2) \approx -0.021 \sin(\pi t^2), \tag{10}$$

gave $H_0 = 284.1 \pm 3$ G for *In*Bi(0.6 at.%). H_0 for the other concentrations was calculated as follows. Previous experiments show that at 1.55-at.% Bi, $\Delta T_c/T_c \approx 7.4\%$,[13] while $\Delta H_0/H_0 \approx 6.5\%$.[14] We therefore assume that

$$\Delta H_0/H_0 = 0.88 \Delta T_c/T_c, \tag{11}$$

and use our measured T_c's to determine H_0 for the other concentrations (Table I). Our calculated value for pure In, $H_0 = 278.2 \pm 3$ G, is in fair agreement with the accepted value[35] of $H_0 = 281.53 \pm 0.06$ G. Using these values of H_0 and the deviation function [Eq. (10)], $H_c(t)$ is known for all concentrations to better than 2% accuracy for $t^2 > 0.5$.

Table I finally contains the results of the resistance measurements, carried out by Pettersen. They were performed on 1-mm-diam wires of 5-cm length. For pure In, only an upper limit of

TABLE I. Experimental parameters of In and *In*Bi spheres.

	Sphere diameter (μm)	λ_0 [a] (Å)	p-to-p tickling field (Oe)	T_c (K)	H_0 [b] (Oe)	$\rho_{4.2}$ ($10^{-7}\Omega$ cm)	RRR ($\rho_{300}/\rho_{4.2}$)	l (μm)
In	18.6	395	0.50	3.4089 ± 0.0002	278.2 (calc.)	<0.005	>16 000	>300
*In*Bi (0.19 at.%)	18.1	510	0.40	3.4051	277.9 (calc.)	3.19	28.2	0.438
*In*Bi (0.395 at.%)	18.8	630	0.46	3.4396	280.4 (calc.)	6.35	14.6	0.220
*In*Bi (0.60 at.%)	17.8	685	0.42	3.4949	284.1 ± 3 (meas.)	9.72	10.0	0.144

[a] Reference 15.
[b] Calculation based on Refs. 13, 14.

ρ was found. The mean-free path l at 4.2 K was computed from ρ using the relationship $\rho_{bulk} l = 5.4 \times 10^{-12}\ \Omega\ \mathrm{cm}^2$ derived from size effect measurements.[36] This gives values of l larger than the free-electron values by a factor of 2.6.

B. Bulk superheating and supercooling fields

Figure 1 shows the results for $\kappa_{sc}(t)$, Eq. (3). Above $t = 0.85$, $\kappa_{sc}(t)$ exhibits a slight, linear decrease with t for all concentrations. The size effect starts around 0.99. Extrapolation to $t = 1$, neglecting the size effect, gives the GL parameter $\kappa(t = 1)$, which is 0.061, 0.155, 0.240, and 0.349, respectively. The uncertainty is 2%, and is due to the uncertainty in H_c. The value in pure In is in excellent agreement with the previous values of 0.062 in single spheres,[5] and 0.060 in powders.[4] Table II contains values of $(1/\kappa)(d\kappa/dt)_1$.

Figure 1 also shows $\kappa_{sh}^{\lambda}(t)$, obtained by inversion of Eq. (1), and from Eq. (6), for pure In. Within the experimental accuracy, it extrapolates to the same value at $t = 1$ as $\kappa_{sc}(t)$. This is not the case for the alloys, for which the use of Eqs. (1) and (6) would lead to $\kappa_{sh}^{\lambda} = 0.119$, 0.164, and 0.206. This shows that Eq. (1) breaks down for finite κ, as expected. In Fig. 2, we have given the superheating results in the form H_{sh}/H_c vs t. Limiting values for H_{sh}/H_c at $t = 1$ are found by extrapolation, again neglecting the size effect. Extrapolation is seen to be straightforward for the alloys, where the temperature variation is slight. In pure In, however, the temperature dependence is strong, and the extrapolation more uncertain. This is so because the nonlocal temperature dependence [Eq. (6)] is valid in In even at $t = 0.99$; so that the region of validity of GL theory, $\Delta t < \kappa^2$, is smaller than the size effect region. This is not the case for the alloys, where in fact the region of validity of GL theory can be read directly from Fig. 2 as being the region of negligible temperature dependence of H_{sh}/H_c. This gives $\Delta t \approx 0.03$, 0.1, and 0.3, respectively, for the alloys, in qualitative agreement with the criterion $\Delta t \approx \kappa^2$. We believe that the pure In sample shows nonideality at $t < 0.9$, but we have every reason to believe that the other samples show ideal superheating down to the lowest temperatures. The constancy of H_{sh}/H_c in the 0.6-at% sample is almost incredible; it changes only by 3% from $t = 0.45$ to $t = 1$.

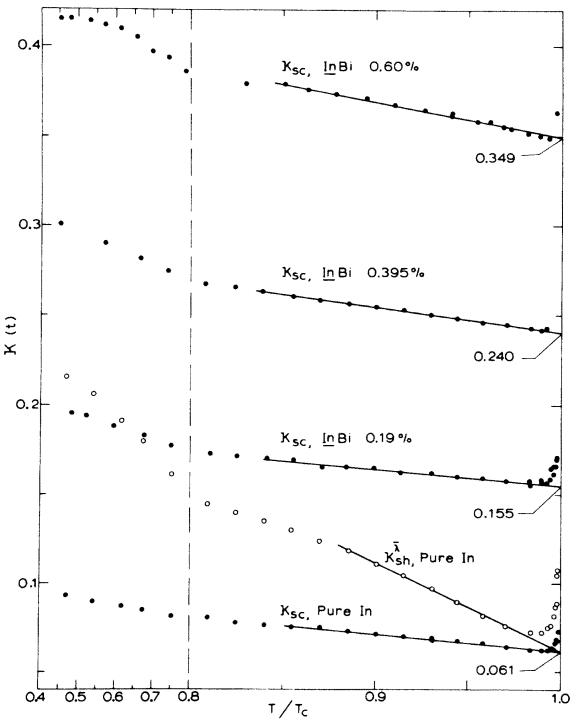

FIG. 1. Supercooling data, given as $\kappa_{sc}(t)$. Temperature dependence is weak and linear, indicating ideal supercooling. Note size effect starting around $t = 0.99$. GL parameter κ is determined by extrapolation to $t = 1$. For pure In, $\kappa_{sh}^{\bar{\lambda}}$, as given by Eq. (1), is included.

Using the extrapolated values of H_{sh}/H_c at $t = 1$, Fig. 3 shows the experimental data compared with the prediction for finite κ, [Eq. (4)]. Again, the uncertainty mainly comes from H_c. The alloys give slightly higher superheating fields than Eq. (4), and pure In a slightly lower value. The extrapolation in pure In may underestimate H_{sh}, however. Referring back to Fig. 2, the broken line shows the extrapolation needed for agreement with Eq. (4); it is entirely credible. In Fig. 3, we have also included data for Sn,[22] β-Ga,[11] and Hg powders.[10] The Sn and β-Ga extrapolations present the same problems as for In. It was concluded earlier[5,11] on the basis of results in In, Sn, and β-Ga that Eq. (1) was good even for finite κ. The present results prove that this conclusion is wrong. From Fig. 3, the experimental results are in fair agreement with Eq. (4) and the numerical calculations.[1,6-8] Equation (1) is good only in the limit $\kappa \to 0$.

Since our values of $\kappa(t = 1)$ are quite accurate, it is interesting to compare them to values derived from the resistivity. Figure 4 shows κ_{expt} and the values computed from the Gor'kov-Goodman relation,[37]

$$\kappa = \kappa_0 + 7.5 \times 10^{-6} \gamma^{1/2} \rho, \tag{12}$$

with $\gamma = 1088$ erg $\mathrm{cm}^{-3}\mathrm{K}^{-2}$ for In.[35] The agreement is seen to be very good: Eq. (12) gives a slope of κ versus concentration which is only 13% lower than the experimental one.

TABLE II. Summary of supercooling and superheating results, extrapolated to $t=1$.

	$\kappa_{sc}(t=1)$	$\frac{1}{\kappa_{sc}}\left(\frac{d\kappa}{dt}\right)_1$	H_{sh}/H_c at $t=1$	$(H_{sh}/H_c)(\kappa_{sc}\sqrt{2})^{1/2}$
Pure In	0.061 ± 0.001	-1.61	3.39 ± 0.07	$1.00\ ^{+0.07}_{-0.03}$
*In*Bi (0.19 at.%)	0.155 ± 0.003	-0.60	2.44 ± 0.05	1.143 ± 0.03
*In*Bi (0.395 at.%)	0.240 ± 0.005	-0.58	2.08 ± 0.04	1.211 ± 0.04
*In*Bi (0.60 at.%)	0.349 ± 0.007	-0.57	1.85 ± 0.04	1.302 ± 0.04

C. Size effect in H_{sh} and H_{sc} near T_c

This size effect was investigated for the *In*Bi 0.19-at.% and 0.395-at.% samples, corresponding to $\kappa=0.155$ and 0.240. The tickling field was reduced to about 0.08 G peak-to-peak, which is about the minimum needed for an adequate signal-to-noise ratio. Measurements were taken up to $\Delta t \approx 2\times10^{-4}$, corresponding to $R/\lambda(T)\approx 6$. At this point, the hysteresis loops closed because of the finite tickling field. To interpret these results, H_c was assumed to be mid-in-between H_{sc} and H_{sh} at the closing point, H_c^{bulk} was then determined from Ref. 1, and T_c determined self-consistently. Figure 5 shows the results. The solid curves have been pieced together from Ginzburg's different limiting expressions.[1] The shrinking hysteresis as the tricritical point is approached is clearly demonstrated, in agreement with experiments on other geometries.[19,25,26]

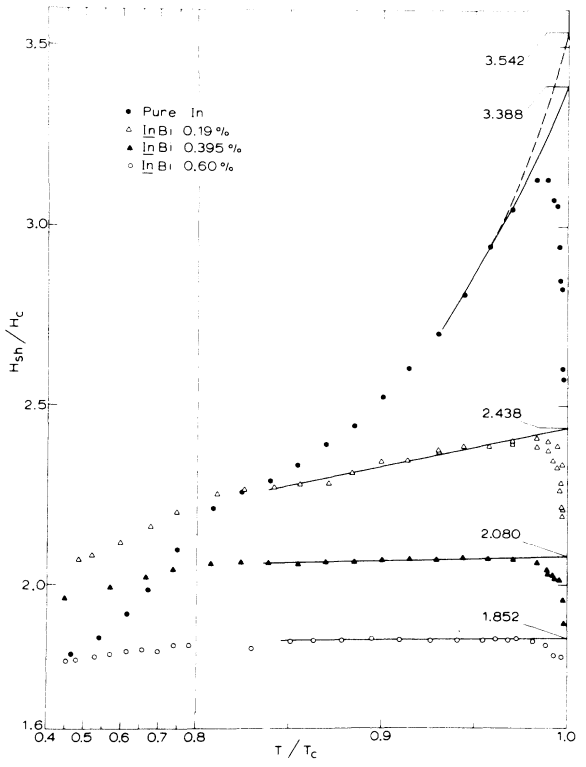

FIG. 2. Superheating data, given as H_{sh}/H_c^{bulk}. Values at $t=1$ are found by extrapolation, neglecting the size effect close to T_c. Broken line for pure In indicates extrapolation necessary to fit Eq. (4). Width of region with no temperature dependence indicates where GL theory is valid for each concentration.

D. Observations of the intermediate state

In the *In*Bi (0.60-at.%) sphere, the IS was observed below $t=0.974$. Above this temperature, the demagnetizing field H_D (Sec. II B) exceeded H_{sc}, and only clean, square hysteresis loops were observed (Fig. 1 of Ref. 15). For the other concentrations, this was the case at all temperatures.

Figure 6 shows a recorder trace of a field sweep at $t=0.864$, with the tickling and static fields parallel. If the field is increased from zero, the transition occurs at H_{sh}. If the sweep is then reversed, the sphere goes into the IS at H_{sc}. At this

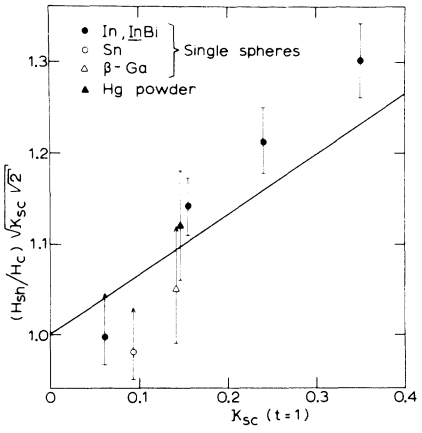

FIG. 3. Deviation of H_{sh} from Eq. (1). Experimental results are in fair agreement with Eq. (4), given by solid line (Hg, β-Ga, and Sn data from Refs. 10, 11, and 22).

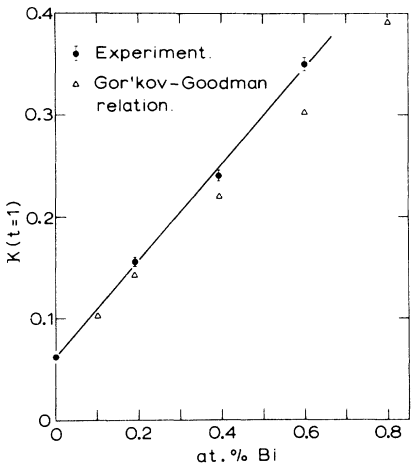

FIG. 4. Experimental values of $\kappa(t=1)$, compared to values derived from the resistivity through Gor'kov-Goodman relation. Agreement is quite good.

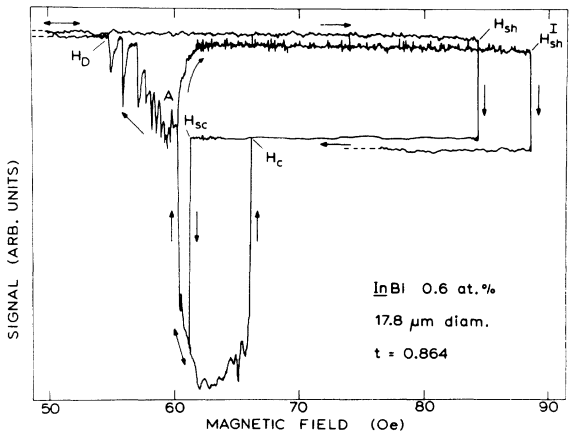

FIG. 6. Recorder trace of field sweep through the intermediate state. Note strong differential paramagnetic effect. When field is increased from A, the sphere stays superheated up to H_{sh}^I, although a flux bundle is frozen in along the polar axis. (See detailed discussion in Sec. IV D.) Slight level difference in the two top curves is due to time drift.

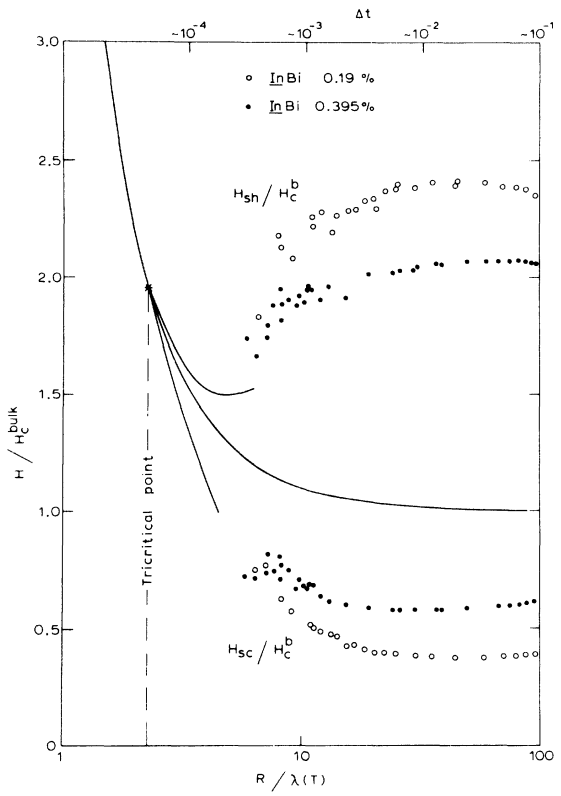

FIG. 5. Size effects in H_{sh}/H_c^{bulk} and H_{sc}/H_c^{bulk} as $T \to T_c$, for two alloys with $\kappa = 0.155$ and 0.240. Solid curves for H_{sc}, H_c, and H_{sh} have been constructed by hand from Ref. 1. Tricritical point could not be reached experimentally, but the approach towards it is clearly seen.

point, we record a strong differential paramagnetic effect. For a small sphere, the amplitude of the differential paramagnetic effect is expected to be somewhat more than twice that of the diamagnetic (Meissner) transition, and this is indeed the case. If the field is again increased from H_{sc}, the sphere goes normal at a field indentified as H_c. This identification is unambiguous: the temperature dependence of this field gives $H_0 = 284.1 \pm 3$ G, with a deviation $D(t^2)$ from a parabola very similar to that of pure In (Sec. IV A).

If the field is instead further decreased from H_{sc}, the flux is expulsed irregularly, until the Meissner state is again reached at H_D. If the field is increased from a value below H_D, the sphere will always reproduce the superheating transition at H_{sh}. If, however, the field is reincreased from the point marked "A," a strange phenomenon occurs. The signal then increases until it has again reached the Meissner level, and the superheating transition occurs at a field $H_{sh}^I > H_{sh}$. Within the experimental accuracy, the transition amplitudes at H_{sh} and H_{sh}^I are the same; one even observes the same slight signal depression close to H_{sh}^I as is observed close to H_{sh} because of the field dependence of the penetration depth (preceding article[15]). Going to lower temperatures, the transitions at H_c and A become continuous and gradual, otherwise there is no change from Fig. 6. What is happening?

Before formulating an answer, more information is provided by looking at the resistive component of the signal, and by looking at the transitions in

perpendicular fields. The signal shown in Fig. 6 is an inductive one: the phase has been optimized to give a maximum Meissner transition signal. In a sweep of the 90°-out-of-phase signal, the transitions at H_{sh}, H_c, and H_{sh}^I all vanish. They are therefore purely inductive. The transitions at H_{sc} and H_D are still there, and there is a lot of structure between H_D and H_c. Thus, there is dissipation connected with the entry and expulsion of flux in the IS between H_D and H_c, but there is *no* dissipation at H_{sh}^I. Still more information is obtained by using a perpendicular static field. There is then no differential paramagnetic effect, in agreement with the IS observations on β-Ga (Fig. 4 of Ref. 11). Otherwise, the features of Fig. 6 are all reproduced, including the transition at H_{sh}^I. However, the transition amplitude at H_{sh}^I is now only about 60% of that at H_{sh}, pointing to a smaller effective superconductive volume[22] V_{eff} at H_{sh}^I than at H_{sh}.

We explain these facts in the following way. We think that the sharp transition out of the differential paramagnetic effect, occurring at A, happens when superconductivity has been reestablished all the way around the equator. Normal flux is then limited to a domain along the polar axis. As the field is reincreased from A, this flux is frozen in, its boundaries do not move with the tickling field, and there is no dissipation. Because the effective demagnetization factor is now much less than for the Meissner state, the applied field can be higher before the equatorial region reaches the ideal superheating field. The NS boundary is close to the poles, and never sees these high fields. In parallel fields, the normal polar regions do not detract measurably from the transition amplitude at H_{sh}^I. In perpendicular fields, however, the tickling field strongly probes these regions, and the amplitude is reduced. Turning this argument around, we can *assume* that at H_{sh}^I, H_{eq} equals the ideal superheating field which is $\approx 1.85\, H_c$. From the observed ratio H_{sh}^I/H_c, this means that $H_{eq}/H_{appl} \approx 1.413$ instead of 1.483 for the Meissner state [Eq. (6)]. This implies that about 14% of the normal-state flux passes through the sphere. Assuming a single flux bundle with an internal field H_c, this gives a bundle diameter of about 7 μm, which agrees well with the estimate from Eq. (9). About 130 flux quanta are enclosed in the bundle. We conclude that we observe ideal superheating in the equatorial region of the sphere, while a bundle of flux simultaneously is frozen in along the polar axis.

Figure 7 finally shows the temperature dependence of the fields H_D and H_c, normalized to H_c^{bulk}. H_D shows a very pronounced size effect: it increases from $0.76H_c$ at $t=0.45$ to $0.85H_c$ at $t=0.975$. This compares with $H_D/H_c = 0.67$ in a large sphere.

From Sec. II, we expect the size effect to be described by a leading term proportional to $[\lambda(T)/R]^{1/2}$. Fitting this to the data, we obtain the solid curve, given by

$$H_D/H_c = 1/k(T) + 1.12[\lambda(T)/R]^{1/2}. \tag{13}$$

The fit is reasonable, but not perfect. The magnitude of the effect agrees well with Landau's[28] and Andrew's[29] predictions, described in Sec. II. H_c, on the other hand, shows almost no size effect at all within the experimental accuracy. In fact, we can put a lower limit of $H_c/H_c^{bulk} \geq 0.96$ at $t=0.9$. This size effect, if present at all, must be smaller by an order of magnitude than the estimates of Sec. II.

V. CONCLUSION

We have carried out precise measurements of the ideal superheating and supercooling fields in 18 μm single spheres of In and *In*Bi (0.19, 0.395, and 0.60 at.%). The extrapolation of $H_{sc}(t)$ determines the GL parameter $\kappa(t=1)$ to 2% accuracy as 0.061, 0.155, 0.240, and 0.349. The Gor'kov-Goodman relation describes this increase in κ quite well. The observed values of H_{sh} are much larger than those given by Eq. (1), which is only valid as $\kappa \to 0$. Our analytical calculation of H_{sh} for finite κ, [Eq. (4)], describes the data fairly well. Finally, we have observed the intermediate state in the *In*Bi (0.6-at.%) sphere, obtaining the first quantitative information on the size effects in H_c and the demagnetizing field H_D, as well as evidence

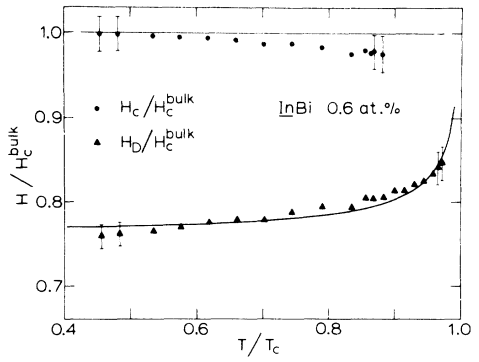

FIG. 7. Temperature dependence of H_D/H_c^{bulk} and H_c/H_c^{bulk} in 17.8-μm, *In*Bi (0.6- at.%) sphere. Strong size effect in the demagnetizing field H_D is well fitted by Eq. (13), solid line. There is virtually no size effect in H_c.

that ideal superheating may take place in a sphere with a frozen-in normal domain. Experiments in progress on materials with higher κ will give more information on the intermediate and mixed state in spheres.

ACKNOWLEDGMENTS

We thank G. Pettersen for carrying out the resistance measurements, and M. R. Esfandiari and H. J. Fink for valuable correspondence.

[1]V. L. Ginzburg, Zh. Eksp. Teor. Fiz. 34, 113 (1958) [Sov. Phys.-JETP 7, 78 (1958)].

[2]*Quantum Fluids*, edited by D. F. Brewer (North-Holland, Amsterdam, 1966), p. 26.

[3]J. Feder, S. R. Kiser, and F. Rothwarf, Phys. Rev. Lett. 17, 87 (1966).

[4]See, for instance, F. W. Smith, A. Baratoff, and M. Cardona, Phys. Kondens. Mater. 12, 145 (1970).

[5]J. Feder and D. S. McLachlan, Phys. Rev. 177, 763 (1969).

[6]J. Matricon and D. Saint-James, Phys. Lett. A 24, 241 (1967).

[7]H. J. Fink and A. G. Presson, Phys. Rev. 182, 498 (1969).

[8]M. R. Esfandiari and H. J. Fink (private communication) and (unpublished).

[9]H. Parr (unpublished).

[10]J. P. Burger, J. Feder, S. R. Kiser, F. Rothwarf, and C. Valette, in *Proceedings of the Tenth International Conference on Low Temperature Physics*, edited by M. P. Malkow (VINITI, Moscow, 1967), Vol. 2B, p. 352.

[11]H. Parr, Phys. Rev. B 7, 166 (1973).

[12]C. Valette and J. P. Burger, J. Phys. (Paris) 30, 562 (1969).

[13]T. Kinsel, E. A. Lynton, and B. Serin, Rev. Mod. Phys. 36, 105 (1964).

[14]I. Kirschner, Phys. Lett. A 47, 139 (1974).

[15]H. Parr, preceding paper, Phys. Rev. B 14, 2842 (1976).

[16]D. Saint-James and P. G. De Gennes, Phys. Lett. 7, 306 (1963).

[17]R. Doll and P. Graf, Phys. Rev. Lett. 19, 897 (1967).

[18]P. Michael and D. S. McLachlan, J. Low Temp. Phys. 14, 607 (1974).

[19]Y. Pellan, J. Blot, J. C. Pineau, and J. Rosenblatt, Phys. Lett. A 44, 415 (1973).

[20]F. W. Smith, A. Baratoff, and M. Cardona, in *Proceedings of the Eleventh International Conference on Low Temperature Physics*, edited by J. F. Allen, D. M. Finlayson, and D. M. McCall (University of St. Andrews, St. Andrews, 1968), Vol. 2, p. 751.

[21]F. London, *Superfluids* (Wiley, New York, 1950), p. 35.

[22]H. Parr, Phys. Rev. B 12, 4886 (1975).

[23]A. M. Goldman, Phys. Rev. Lett. 30. 1038 (1973).

[24]M. R. Esfandiari and H. J. Fink, in *Proceedings of the Fourteenth International Conference on Low Temperature Physics*, edited by M. Krusius and M. Vuorio (North-Holland/American, Elsevier, 1975), Vol. 2, p. 187. Figure 3 has been revised by the authors.

[25]D. S. McLachlan, J. Low Temp. Phys. 6, 385 (1972).

[26]D. S. McLachlan, Solid State Commun. 8, 1589 (1970).

[27]L. Landau, Phys. Z. Sowjetunion 11, 129 (1937).

[28]L. Landau, J. Phys. USSR 7, 99 (1943).

[29]E. R. Andrew, Proc. R. Soc. A 194, 98 (1948).

[30]V. L. Ginzburg, Physica (Utr.) 24, S42 (1958).

[31]M. Tinkham, *Introduction to Superconductivity* (McGraw-Hill, New York, 1975), p. 95.

[32]Alloys prepared from 99.9999% In and Bi by the Central Institute of Industrial Research, Oslo. The concentration was determined by x-ray fluorescence spectrometry.

[33]H. Parr, Phys. Rev. B 10, 4572 (1974). See especially Fig. 2.

[34]R. C. Carriker and C. A. Reynolds, Phys. Rev. B 2, 3991 (1970).

[35]D. U. Gubser, D. E. Mapother, and D. L. Connelly, Phys. Rev. B 2, 2547 (1970).

[36]K. Førsvoll and I. Holwech, Philos. Mag. 10, 181 (1964).

[37]B. B. Goodman, IBM J. Res. Dev. 6, 63 (1962).